



Big Data-Driven Decision Support System Framework for Sustainable Multi-Criteria Computing in Green Systems

Downloaded from: <https://research.chalmers.se>, 2025-12-26 05:27 UTC

Citation for the original published paper (version of record):

Mokarram, M., Najafi, A., Aghaei, J. et al (2026). Big Data-Driven Decision Support System Framework for Sustainable Multi-Criteria Computing in Green Systems. *Big Data Mining and Analytics*, 9(1): 103-118.
<http://dx.doi.org/10.26599/BDMA.2025.9020040>

N.B. When citing this work, cite the original published paper.

Big Data-Driven Decision Support System Framework for Sustainable Multi-Criteria Computing in Green Systems

Mohammad Jafar Mokarram, Arsalan Najafi, Jamshid Aghaei, and Meng Yuan*

Abstract: Big data provide valuable insights by offering diverse information and sophisticated analysis through advanced algorithms. However, its huge volume, variety, and speed present significant challenges for effective computing. To address these, this study applies a Multi-Criteria Decision-Making (MCDM) framework to manage spatial big data, specifically in new green applications. The paper introduces a robust MCDM framework using big data, designed to address renewable energy challenges within the environmental sector. This framework systematically prioritizes and evaluates large environmental datasets, incorporating economic, environmental, and social factors. This framework is especially efficient and reliable for green energy initiatives. Moreover, a pre-processing step extracts key features to enable high-performance efficient analysis and visualization. Results show that the framework improves accuracy by 18% compared to conventional single-criterion data analysis approaches in a large-scale case study and provides system managers with an interactive 3D visualization tool to enhance decision making process in big data environmental management.

Key words: big data management; Fuzzy Best Worst Method (Fuzzy-BWM); green system; visualization

1 Introduction

The global electricity demand has witnessed a substantial surge due to population growth, urbanization, and increased reliance on electronic devices^[1]. However, a significant challenge persists, particularly in less developed areas, where electricity shortages hinder socio-economic development. The scarcity of electricity in these regions not only impedes basic daily activities, but also limits access to crucial services^[2]. Therefore, it is essential to investigate and employ innovative methods of producing electricity. The distinctive qualities of renewable energy sources

offer a viable route for the production of sustainable and dependable power, whereas traditional energy sources, which are typified by fossil fuels and greatly contribute to environmental deterioration, air pollution, and climate change^[1]. Renewable energy sources, such as solar, wind, biomass, and hydrogen, offer sustainable solutions to the electricity shortage. The use of these new energy technologies helps to meet the growing demand for electricity and, at the same time, ensures a cleaner and more environmentally friendly approach to power generation^[3]. In the realm of renewable energy sources, hydrogen stands out as a

-
- Mohammad Jafar Mokarram and Meng Yuan are with College of Mechatronics and Control Engineering and College of Computer Science and Software Engineering, Shenzhen University, Shenzhen 518060, China. E-mail: m.j.mokarram@gmail.com; yuanmengszu@gmail.com.
 - Arsalan Najafi is with Department of Architecture and Civil Engineering, Chalmers University of Technology, Gothenburg 41258, Sweden. E-mail: Arsalan.najafi@chalmers.se.
 - Jamshid Aghaei is with School of Engineering and Technology, Central Queensland University, Rockhampton 4701, Australia. E-mail: j.aghaei@cqu.edu.au.

* To whom correspondence should be addressed.

Manuscript received: 2024-11-09; revised: 2025-03-20; accepted: 2025-04-07

promising candidate for sustainable electricity generation^[4], while mitigating the environmental impact of power generation^[5]. Hydrogen, often referred to as the “fuel of the future”, can be produced through various methods, such as electrolysis, where water is split into hydrogen and oxygen using an electric current^[6], or through the reforming of natural gas^[7]. Despite their potential, challenges like energy input requirements and infrastructure development have tempered their widespread adoption. On the other hand, producing hydrogen through biomass, especially in undeveloped areas, has emerged as a promising method^[8]. Biomass, derived from organic materials, such as plant and animal waste, agricultural residues, and dedicated energy crops, presents a compelling solution. Unlike some renewable sources, biomass offers a reliable and consistent energy supply, with the added benefit of utilizing existing infrastructure.

On the other hand, considering environmental aspects is vital when considering hydrogen from biomass. Environmental data are often considered big data due to their extensive nature and spatial and temporal dispersion. These data are collected from various geographical sources over extended periods, which leads to an increase in both volume and diversity. Additionally, many different types of parameters are needed to account for the multiple aspects involved in environmental analysis, further contributing to the complexity of big data^[9, 10]. To manage and analyze this type of data, advanced computing tools are necessary^[11]. These tools must not only possess high processing power, but also be designed within the framework of big data environmental green computing^[12]. The importance of applying optimal methods in environmental data processing is critical because these data directly influence the health of the environment and the quality of human life. Inaccurate or incomplete analysis can lead to incorrect decisions with negative consequences for ecosystems and communities. Therefore, modern analytical tools and methods, such as big data mining, artificial intelligence, and multi-criteria decision-making, are essential for effective environmental big data analysis.

Numerous studies have explored different aspects of the placement of renewable energy. A robust framework in micro grid application has been developed in Ref. [13]. The placement of distributed

generation in deregulated electricity markets has also been investigated in Ref. [14]. In addition, a review has focused on the optimal placement of distributed generation, when they focus on minimizing power losses and the enhancement of voltage stability in distribution systems^[15]. Although these studies have made significant contributions, optimizing renewable energy deployment requires a more comprehensive approach that includes spatial analysis. This approach is essential to consider geographical, environmental, and socioeconomic factors that can significantly influence the efficiency and effectiveness of renewable energy systems^[16]. Without spatial big data analysis, solutions may not optimize resource use or fully achieve broader sustainability goals. To deal with, a methodological framework for spatial modeling of hydrogen demand in cities has been proposed but does not utilize Multi-Criteria Decision-Making (MCDM). In such a complex field, MCDM plays a crucial role in achieving better outcomes by incorporating various parameters that impact the results and ensuring more accurate and robust models^[17].

While neural network approaches, such as Long Short-Term Memory (LSTM)^[18] and Convolutional Neural Networks (CNN)^[19], have been widely applied in energy-related predictive modeling, they exhibit limitations for sustainable hydrogen production site selection. LSTM excels at time-series forecasting, such as energy demand prediction^[1], and CNN aids in spatial feature extraction and interpretability^[20]. However, these methods struggle to integrate heterogeneous, multi-criteria environmental data without extensive preprocessing or hybrid designs. For instance, advanced architectures like MU-Net-optLSTM leverage spatial-temporal data for real-time monitoring^[21], but their focus on classification limits their utility in holistic decision-making. Similarly, models like GLE-SVR for DNI estimation^[22] and federated approaches like ResFed^[23] optimize predictions on edge devices, yet lack the transparency and multi-factor synthesis required for green energy planning. Moreover, their opaque decision-making processes and high computational demands can hinder practical decision-support in resource-constrained settings. In contrast, MCDM methods offer a promising avenue to address these challenges by systematically evaluating diverse factors.

There are some methods in weighting criteria for

MCDM problems, each presenting distinct strengths and advantages^[24]. Notable among these methods are the Analytic Hierarchy Process (AHP)^[25] and the Analytic Network Process (ANP). AHP stands out for its structured approach which systematically breaking down complex decisions into hierarchical structures. ANP, on the other hand, extends the capabilities of AHP by incorporating interdependencies between criteria. This enables it to capture complex relationships between parameters^[26]. Regression analysis, a statistical method, adopts a data-driven approach by leveraging historical data to identify influential factors^[11]. Another effective methodology is the Technique for Order of Preference by Similarity to Ideal Solution (TOPSIS)^[27]. In contrast, the Best Worst Method (BWM) introduces a unique approach by simultaneously considering both the best and worst criteria^[28, 29]. However, upon comparing BWM with the ANP and AHP, certain drawbacks come to light^[30]. ANP may encounter challenges in managing complex interdependencies which leads to increase computational complexity and potential model instability. Similarly, the AHP has its limitations, including sensitivity to changes in the number of criteria and constraints^[31]. In fact, BWM excels in providing a systematic, transparent, and less biased approach to weight assignment^[32]. Moreover, the application of the fuzzy method in this study is proved crucial for homogenizing data with varying units. Moreover, it facilitates the representation of suitable locations on a scale from 1 to 0, with 1 indicating high suitability and 0 denoting unsuitability^[33].

It should be noted that in MCDM problems, accurately representing spatial data is often paramount for effective decision-making. However, obtaining measurements at all places is impractical or sometimes impossible due to various constraints, such as cost, accessibility, or physical limitations. To overcome this challenge, interpolation methods are employed to estimate values at unmeasured locations based on available data. Among these methods, Inverse Distance Weighting (IDW)^[34], Kriging, and spline methods are well-known. As a geostatistical technique, Kriging offers a robust framework for capturing spatial dependencies. Unlike deterministic methods, such as IDW or spline interpolation, Kriging integrates statistical models of spatial correlation^[35]. By utilizing a semivariogram to quantify and model these correlations, Kriging ensures that the predictions are

not only smooth but also statistically reliable^[36]. Moreover, the IDW method, particularly in areas with sparse data generates oversmoothed surfaces^[37].

Another important aspect of a comprehensive assessment is to investigate the effect of different climates on biomass-based hydrogen production. Climate influences resource availability, process efficiency, environmental big data impact, and the overall sustainability of hydrogen production. For example, a least-cost geospatial modeling approach has been applied to hydrogen production in Ref. [17], although the authors focused mainly on economic aspects, they overlooked the impact of different climates. Similarly, a spatial assessment of land suitability has been conducted to address the insecurity of ecosystem services, but does not integrate advanced methodologies or broader considerations, like energy production^[25]. In fact, understanding how varying climates influence these processes is crucial for developing more accurate and sustainable strategies.

Based on the reviewed literature, significant gaps in this field include the need for further investigation into hydrogen production from biomass gasification, especially in underdeveloped regions where inputs for electrolysis and reforming gas are challenging to obtain. Another gap is the limited use of spatial analysis, particularly through MCDM methods that consider various influencing factors. In addition, the creation of maps using interpolation techniques is essential to visualize potential production sites by estimating hydrogen yields across different regions, even in areas with sparse data. While various renewable energy sources, such as solar, wind, and hydro, offer significant potential^[22], this study focuses exclusively on biomass-based renewable energy due to the region's high agricultural potential. To maximize the efficiency of renewable energy usage, it is essential to align energy sources with the available local potential.

(1) Integration of spatial analysis with fuzzy-BWM: The study develops a hybrid framework that uniquely combines spatial methodologies with the Fuzzy-BWM for the first time in the context of hydrogen production site selection. This integration allows for a more precise and reliable evaluation of potential sites by accounting for both spatial variability and decision-maker preferences, which are often treated separately in traditional approaches.

(2) Use of interpolation maps for visualizing

hydrogen distribution: The study also introduces the innovative use of interpolation maps to visually represent the distribution of hydrogen potential across different regions. This geospatial visualization technique enhances the understanding of where hydrogen production would be most effective.

(3) Comparative analysis across diverse climatic regions: Unlike previous studies that tend to focus on specific regions or climates, this research conducts a comprehensive comparative analysis across moderate and semi-arid climates.

This paper is organized into four sections. Section 2 details the materials and methods, covering Kriging, Fuzzy, and the BWM. It also explains how hydrogen production from biomass gasification and electricity generation from hydrogen are quantified. Section 3 presents the results that include case study and data description, followed by an analysis of hydrogen production and its byproducts. The section also explores the correlation between climate parameters and hydrogen production, and assesses electricity generation from hydrogen. Section 4 concludes the paper and offers suggestions for future research.

2 Material and Method

In this section, the methodology employed in this study is detailed, covering the Kriging method in Section 2.1, the Fuzzy method in Section 2.2, and the BWM in Section 2.3. Subsequently, hydrogen production is quantified in Section 2.4. Finally, the amount of electricity generation available from hydrogen is explained in Section 2.5.

2.1 Ordinary Kriging method

Ordinary Kriging is chosen as the interpolation method for this study due to its suitability for the data type and research objectives. Given the spatial variation in hydrogen production data without a clear global trend, ordinary Kriging is considered an appropriate choice over more complex methods like universal Kriging. This method is robust, does not assume a global mean, and is particularly effective for capturing local variations when the spatial process is stationary^[38]. The ordinary Kriging formulation is presented as follows^[39]:

$$Z(u) = \lambda + \sum_{i=1}^n \omega_i (Z(u_i) - \lambda) \quad (1)$$

where $Z(u)$ is the estimated value at the unsampled

location u and λ is the global mean of the variable. Also, $Z(u_i)$ is the observed value at the sampled location u_i , ω_i is the Kriging weight assigned to each observed value, and n is the number of sampled points within the specified neighborhood.

The weights are determined based on the spatial autocorrelation structure, and the Kriging method aims to minimize the estimation error by assigning higher weights to nearby points that exhibit a stronger correlation with the unsampled location.

It should be noted that in this study, various semivariogram models, including exponential, Gaussian, and spherical models, are evaluated. The selection of the best model is based on the Root Mean Square Error (RMSE), calculated as follows:

$$\text{RMSE} = \sqrt{\frac{1}{n} \sum_{i=1}^n (Z(u_i) - \hat{Z}(u_i))^2} \quad (2)$$

2.2 Fuzzy method

This paper employs membership functions within the fuzzy method framework to homogenize the input data and facilitate subsequent big data analysis. This involves mapping input data points to linguistic terms (e.g., small, medium, and large) using a fuzzy inference system. It should be noted that, the selection of specific membership functions is guided by the inherent characteristics of the input data. For example, parameters, such as Calcium Carbonate Equivalent (CCE) or slope, which negatively impact biomass and hydrogen production, are modeled using small membership functions^[40]. Conversely, large membership functions are utilized for parameters like maximum temperature and rainfall, which positively influence biomass and hydrogen production^[41]. The degree of membership within each fuzzy set is then calculated as bellow^[42]:

$$\text{Large}(x) = \begin{cases} \frac{1}{1 + \left(\frac{x}{\text{Threshold}}\right)^2}, & \text{if } x \geq \text{threshold}; \\ 0, & \text{otherwise} \end{cases} \quad (3)$$

$$\text{Small}(x) = \begin{cases} 1 - \frac{1}{1 + \left(\frac{x}{\text{Threshold}}\right)^2}, & \text{if } x < \text{threshold}; \\ 0, & \text{otherwise} \end{cases} \quad (4)$$

For parameters, such as sunshine, rainfall, average temperature, maximum temperature, and PH, Eq. (3) is

employed. Meanwhile, for parameters, such as minimum temperature, CCE, elevation, slope, Electrical Conductivity (EC), and soil texture, Eq. (4) is utilized to define the membership function. The threshold values for Eqs. (3) and (4) are chosen based on Ref. [43] and presented in Table 1.

During the fuzzification process applied to the maps, optimal classes are designated with the numerical value of 1 for the most suitability. On the other hand, unsuitable classes are assigned a numerical value of 0 to represent a lack of appropriateness.

2.3 BWM

As stated, the BWM is utilized to evaluate and rank alternatives based on multiple criteria. The BWM entails pairwise comparisons where decision-makers assess criteria to determine the best and worst among them. These comparisons yield valuable data on the relative significance of each criterion. Subsequently, mathematical models are employed to compute the weights of the criteria based on the outcomes of the pairwise comparisons^[44]. In the following, the procedures of the BWM method are explained in five steps^[45]:

(1) Identifying decision criteria: In this step the criteria that are needed to be used in the BWM are defined.

(2) Selecting the best and worst criteria: Determining the most important (best) criterion, denoted as *B*, and the least important (worst) criterion, denoted as *Z*.

(3) Pairwise comparison with *B*: Comparing the best criterion against all other criteria using a scale ranging from 1 to 9. The resulting vector is

$c_B = (c_{B1}, c_{B2}, \dots, c_{Bn})$, where $c_{BB} = 1$ and the best criterion is compared to itself.

(4) Pairwise comparison with *Z*: Similarly, comparing all criteria against the worst criterion using the same scale, yielding $c_Z = (c_{1Z}, c_{2Z}, \dots, c_{nZ})$, where $c_{ZZ} = 1$ for the same reason.

(5) Weight calculation: Assigning weights to the criteria based on these comparisons.

In the BWM method, optimal weights are determined by minimizing the maximum deviation in pairwise comparisons. This is done by evaluating the comparison ratios between the best criterion *B*, the worst criterion *Z*, and the remaining criteria *j*, for all *j*. The optimal weight for any comparison between the best and other criteria, or between the worst and other criteria, is given by

$$c_{Bj}^* = \frac{z_B}{z_j}, \quad j = 1, 2, \dots, n \tag{5}$$

$$c_{jZ}^* = \frac{z_j}{z_Z}, \quad j = 1, 2, \dots, n \tag{6}$$

The objective is to minimize the largest deviation between the actual comparison ratios and the provided comparison values. Mathematically, this is represented as minimizing the maximum of the following terms:

$$\begin{aligned} \min \max_j \left\{ \left\| \frac{z_B}{z_j} - c_{Bj} \right\|, \left\| \frac{z_j}{z_Z} - c_{jZ} \right\| \right\}, \\ \text{s.t., } \sum_{j=1}^n z_j = 1, z_j \geq 0, \text{ for all } j \end{aligned} \tag{7}$$

This problem can be simplified into a linear model,

$$\left\| \frac{z_B}{z_j} - c_{Bj} \right\| \leq \xi, \quad \text{for all } j \tag{8}$$

Table 1 Threshold values for each parameter.

Parameter	Highly suitable	Moderately suitable	Marginally suitable	Not suitable
Annual minimum temperature (°C)	16–18	14–16	14–12	<12
Annual maximum temperature (°C)	24–28	28–32	32–36	>36
Elevation (m)	<1700	1700–2000	2000–2300	>2300
Slope (%)	0–2	2–6	6–12	>12
pH	6.5–7.5	5.8–6.5, 7.5–7.8	5.5–5.8, 7.8–8.2	<5.5, >8.2
EC (dS/m)	0–4	4–6	6–8	>8
CCE (%)	0–15	15–30	30–50	>50
Soil texture	Loam, clay loam, sandy clay, clay	Sandy loam, sandy clay loam	Loam sandy, silty loam, silty clay loam	Silty clay, sandy and silty
Rainfall (mm)	>350	350–250	250–200	<200
Organic carbon (OC) (%)	>2	1–2	0.5–1	<0.5

$$\left\| \frac{z_j}{z_Z} - c_{Zj} \right\| \leq \xi, \quad \text{for all } j \quad (9)$$

$$\sum_{j=1}^n z_j = 1, \quad z_j \geq 0, \quad \text{for all } j \quad (10)$$

When multiple criteria are involved and the optimal value ξ^* is non-zero, the problem may yield several feasible weight distributions. To find the minimum and maximum possible weights for each criterion, the following linear programming problems are solved:

Minimization problem:

$$\begin{aligned} & \min Z_j, \\ \text{s.t.}, & \quad \|Z_B - c_{Bj}Z_j\| \leq \xi^* Z_j, \\ & \quad \|Z_j - c_{jZ}Z_Z\| \leq \xi^* Z_Z, \\ & \quad \sum_{j=1}^n Z_j = 1, \quad Z_j \geq 0, \quad \text{for all } j \end{aligned} \quad (11)$$

Maximization problem:

$$\begin{aligned} & \max Z_j, \\ \text{s.t.}, & \quad \|Z_B - c_{Bj}Z_j\| \leq \xi^* Z_j, \\ & \quad \|Z_j - c_{jZ}Z_Z\| \leq \xi^* Z_Z, \\ & \quad \sum_{j=1}^n Z_j = 1, \quad Z_j \geq 0, \quad \text{for all } j \end{aligned} \quad (12)$$

It should be noted that, in the minimization problem, the goal is to find the smallest possible weight for each criterion. While, in the maximization problem, the objective is to find the largest possible weight for each criterion, while still satisfying the same set of constraints. The optimal weight for each criterion Z_j^* is then computed as the average of the minimum and maximum weights obtained from these models,

$$Z_j^* = \frac{Z_j^{*\min} + Z_j^{*\max}}{2} \quad (13)$$

Finally, the consistency of the model is evaluated using the Consistency Ratio (CR), which measures the degree of reliability in the pairwise comparisons. The consistency ratio is given by

$$\text{Consistency ratio} = \frac{\xi^*}{\text{Consistency index}} \quad (14)$$

The consistency index is available in Ref. [46], and helps verify whether the comparisons are consistent or need adjustment.

2.4 Quantifying hydrogen production from biomass gasification

Hydrogen production via biomass gasification offers key advantages over methods, like electrolysis or gas reforming, particularly in terms of sustainability. Biomass can achieve carbon neutrality as the carbon dioxide released during gasification is offset by the amount absorbed during plant growth^[47]. This makes it a low-carbon alternative, especially compared to gas reforming. Another advantage of biomass gasification is its ability to produce multiple valuable outputs, including hydrogen, methane, and syngas. Additionally, it is a cost-effective and straightforward process for hydrogen generation, especially for regions lacking access to water or gas resources^[48]. Gasification is a thermochemical conversion process that converts biomass into syngas, a mixture of hydrogen, carbon monoxide, methane, carbon dioxide, and other hydrocarbons. This process is typically carried out at high temperatures (700–1200 °C) and pressures (1–20 bar) in a gasifier^[49]. The efficiency of gasification for hydrogen production is typically between 10% and 30%. This means that for every 100 megajoules (MJ) of energy in the biomass, 10–30 MJ is released in the form of hydrogen gas^[50, 51],

$$H_2 = BY \times (0.10 - 0.30 \times \text{BEC}) \quad (15)$$

$$\text{Methane} = BY \times (0.05 - 0.10 \times \text{BEC}) \quad (16)$$

$$\text{Tar} = BY \times (0.025 - 0.05 \times \text{BEC}) \quad (17)$$

$$\text{Char} = BY \times (0.30 - 0.40 \times \text{BEC}) \quad (18)$$

$$CO_2 = BY \times (0.10 - 0.20 \times \text{BEC}) \quad (19)$$

where BY denotes biomass yield (t/ha) and BEC denotes biomass energy content (MJ/t).

2.5 Electricity generation from hydrogen

In this section, we focus on efficiently converting hydrogen into electricity using a fuel cell system. The efficiency of a fuel cell plays a pivotal role in determining the overall performance and viability of such systems. Fuel efficiency, denoted as η , represents the ratio of the useful energy output of the fuel cell system to the energy input from the fuel source^[52]. It is typically expressed as a percentage and encompasses losses incurred during various conversion processes. To begin, the fuel efficiency of the chosen fuel cell system is evaluated^[53]. This efficiency factor is utilized

in subsequent calculations to estimate the electricity generation potential of the system. The primary objective is to convert the energy content of hydrogen, produced in MJ, into megawatt-hours (MWh) of electricity. The methodology employed for calculating the electricity generated from hydrogen can be summarized as follows:

(1) The fuel efficiency (η) of the fuel cell system is initially analyzed and established at 60% in this paper. This efficiency factor accounts for losses during the conversion of hydrogen to electricity.

(2) The energy content of hydrogen (E_{H_2}) is converted from MJ to MWh. This conversion is performed using a conversion factor of 0.000 277 778 kWh/MJ as

$$E_{H_2}(\text{MWh}) = E_{H_2}(\text{MJ}) \times \frac{0.000277778 \text{ kWh}}{\text{MJ}} \times \frac{1 \text{ MWh}}{1000 \text{ kWh}} \quad (20)$$

(3) The electricity generated ($E_{\text{electricity}}$) is determined by multiplying the energy content of hydrogen in MWh by the fuel cell efficiency (η) as

$$E_{\text{electricity}} = E_{H_2} \times \eta \quad (21)$$

Using this comprehensive big data approach, electricity generation can be estimated based on hydrogen levels within the fuzzy-BWM method.

3 Result

In this section, the results of the proposed framework are presented. Firstly, the case study and data description are provided in Sections 3.1 and 3.2, respectively. Section 3.3 investigates hydrogen production through gasification, and Section 3.4 provides the byproducts of the gasification process, including tar, char, and carbon dioxide. Finally, the correlation between hydrogen production and climate parameters is provided in Section 3.5, and the electricity generation assessment from hydrogen is provided in Section 3.6.

3.1 Case study

The study area is carefully selected to encompass two distinct climate zones within Iran’s southwest region, specifically located in Fars province. The purpose is to

conduct a thorough examination of diverse climatic conditions affecting biomass hydrogen production. As depicted in Table 2, the study area exhibits a significant elevation range, reaching its peak at 3172 m in the northern sector of Case 1. In contrast, the lowest elevation lies in the eastern section, specifically in Case 2, at an altitude of 1518 m. Each of these regions possesses unique climatic characteristics, concisely summarized as follows:

Case 1: This region features an average annual rainfall of 365 mm, accompanied by temperature extremes ranging from a maximum of 37°C to a minimum of 2°C below zero (<https://www.farsmet.ir>).

Case 2: This case has a distinctly warm climate with a slightly humid environment. Summer temperatures can soar to a maximum of 42°C, while winter temperatures may descend to 2°C. The average annual rainfall in this region falls within the range of 191 mm (<https://www.farsmet.ir>).

Further details about each of the study areas are tabulated in Table 2.

3.2 Data description

The analysis is conducted by incorporating a diverse set of big environmental climatic data, topographical insights, and soil characteristics. The input parameters include EC, CCE, pH, soil texture components (clay, sand, and silt), temperature extremes (T_{max} and T_{min}), average temperature (T_{average}), rainfall, slope, and elevation. To obtain precise climatic data, information has been obtained from the meteorological department of Fars province, accessible at <https://www.farsmet.ir>. In consideration of topographical elements, the study relies upon topographical maps sourced from the United States Geological Survey (USGS). To assess soil characteristics, samples are meticulously collected from 30 different points within the study cases. Moreover, Table 3 provides a detailed summary of the key soil properties essential to the analysis.

The steps of the research are shown in Fig. 1.

3.3 Quantitative analysis of hydrogen production through gasification

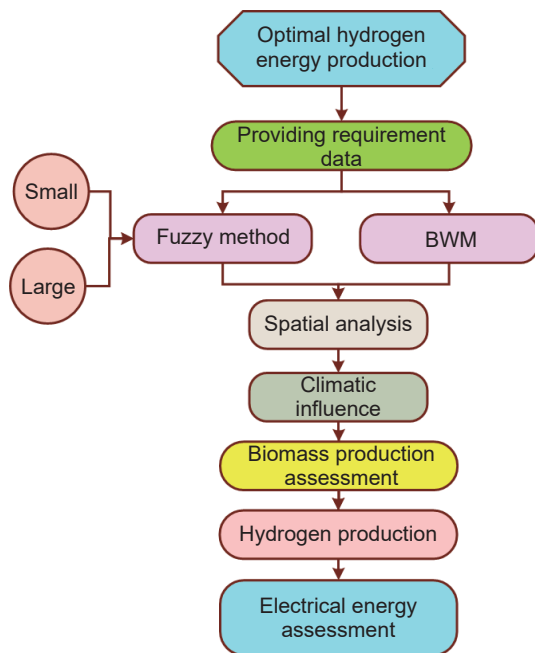
Hydrogen can be extracted from biomass using various

Table 2 Characteristics of studied cases.

Case	Latitude	Longitude	Area (km ²)	Elevation (m)	Name
1	53° 30' to 54° 01'	29° 11' to 29° 24'	1737.63	1518–3172	Marvdasht
2	52° 01' to 52° 48'	29° 36' to 30° 18'	2361.06	1566–2891	Darab

Table 3 Descriptive statistics for key variables.

Case	Statistic	CCE	Sunshine (h)	Rainfall (mm)	Slope (%)	Elevation (m)	Clay (%)	Sand (%)	Silt (%)	OC (%)	pH	EC (dS)
Case 1	Average	42.75	3361.72	298.89	9.92	1646.06	33.29	40.99	25.69	1.04	7.60	5.59
	Minimum	20.72	3196.02	207.99	0.11	369.00	23.14	23.63	8.10	0.71	7.30	0.00
	Maximum	52.42	3495.48	604.74	48.17	2886.00	48.71	59.86	38.10	1.81	7.77	28.93
	Standard deviation	7.83	71.65	86.97	10.30	573.85	4.69	7.32	5.05	0.25	0.07	8.24
	Range	31.70	299.46	396.75	48.06	2517.00	25.57	36.23	29.00	1.10	0.47	28.93
Case 2	Average	47.21	3465.67	238.86	8.18	1478.56	32.67	45.47	21.88	0.74	7.64	3.61
	Minimum	44.67	3441.67	219.96	0.25	1058.00	25.74	30.02	14.43	0.71	7.64	1.87
	Maximum	49.70	3495.48	258.65	35.91	2257.00	47.97	55.62	30.12	0.75	7.66	9.58
	Standard deviation	1.33	17.25	13.75	9.42	345.51	6.42	6.92	3.47	0.01	0.00	1.72
	Range	5.03	53.81	38.69	35.66	1199.00	22.23	25.60	15.69	0.04	0.02	7.71

**Fig. 1** Proposed framework for optimal big data allocation of hydrogen production.

techniques, with thermochemical processes like gasification and pyrolysis being prominent examples^[54]. Gasification involves converting biomass into syngas, which contains hydrogen, tar, char, carbon monoxide, and other components^[55, 56]. By separating the syngas, high-purity hydrogen can be produced. Notably, biomass gasification is environmentally friendly and carbon-neutral^[57, 58]. It should be noted that it aligns to address climate change, while mitigating electricity shortages through sustainable energy solutions^[59, 60].

To apply the fuzzy method for each parameter in accordance with Table 1, threshold values are utilized. For parameters such as rainfall or sunshine, where

higher values are associated with increased yield and biomass production, large membership functions are assigned. In these instances, as values increase, the membership function converges towards 1. Conversely, for parameters like minimum temperature, smaller membership functions are employed, as a decrease in minimum temperature leads to diminished performance (with decreasing values causing the membership function to approach 0). As a result, all parameter values are normalized between zero and one. Proximity to 1 indicates a positive impact on biomass and hydrogen production performance, while values approaching zero signify a negative influence of the input parameter on biomass and hydrogen production performance.

The subsequent phase involved refining and assigning weights to input parameters using the BWM. The results of this weighting process play a crucial role in quantifying subsequent hydrogen production levels. In the BWM process, precision at each sampling point is enhanced through a comprehensive two-by-two comparison for each parameter. This involves soliciting input from 20 field experts, who assess the weight of each parameter based on the current situation and the necessary elements for optimal growth. The obtained results of BWM method are then extracted and provided in Fig. 2. As illustrated in Fig. 2, the weights derived from the BWM underscore the significance of various factors in hydrogen production. For instance, sunshine is the most effective parameter and substantial weight is 0.3. In contrast, the soil texture exhibits the lowest weight, approximately 0.024.

After weighing each parameter using the BWM, we can employ Eq. (15) to quantify the hydrogen content

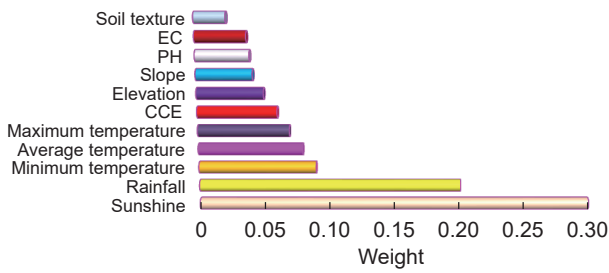


Fig. 2 Weight of each criterion using BWM.

at each sample point. Based on the results, in Case 1, hydrogen production ranges from 0 to 192 MJ, while in Case 2, it varies between 0 to 1575 MJ. To verify the accuracy of the hydrogen maps produced in the two study areas, the yield rate assessment is carried out. The Receiver Operator Characteristic (ROC) curve and the precision-recall curve visually represent the trade-off between sensitivity and specificity as depicted in Figs. 3 and 4, respectively.

According to Fig. 3 and Table 4, the Area Under Curve (AUC) value is 0.864 and it approves the applicability of the fuzzy-BWM in identifying regions with varying hydrogen yields, which illustrates a balance between sensitivity (true positive rate) and specificity (1–false positive rate, where “1–” represents the complement of the false positive rate, indicating the true negative rate). The curve closely follows the top-left corner of the plot, suggesting a high level of discriminative ability. This indicates that the method performs well in distinguishing between high- and low-yield areas while minimizing false positives. On the other hand, the precision-recall curve, with an AUC

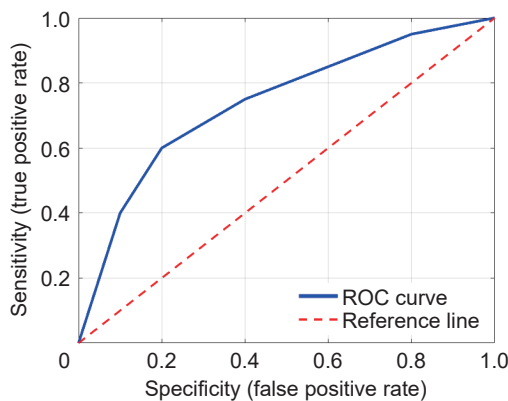


Fig. 3 Specificity and sensitivity results (ROC curve).

Table 4 Obtained results related to ROC method.

AUC	Standard error of AUC	Asymptotic significant of AUC	95% confidence interval lower bound of AUC	95% confidence interval upper bound of AUC
0.864	0.131	0.016	0.608	1.000

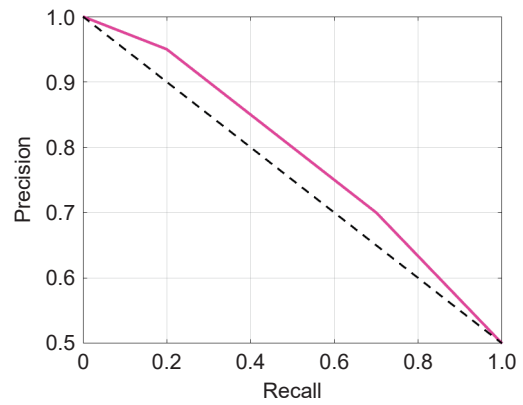


Fig. 4 Precision-recall curve.

value of 0.84, provides additional insights into the method’s performance. Based on Fig. 4, the start precision is 1.0 and it decreases to 0.5.

3.4 Byproducts of the gasification process

As stated, hydrogen constitutes the predominant component of production in the gasification process. However, other byproducts emerge during this process. In this paper, the byproduct amount is also investigated as below.

(1) Methane

The quantification of methane production from biomass during the gasification process is detailed in Eq. (15). Subsequently, interpolation maps are generated utilizing Kriging method for each investigated case (see Fig. 5).

Figure 5 depicts three different parts of each cases including northern, central, and southern parts of the study area for methane production in MJ. In Case 1, the results indicate that the northern regions exhibit significantly high methane production levels with approximately 15 MJ production. In contrast, the southern regions show much lower production values, with levels dropping to less than 4 MJ. In Case 2, a greater variation in energy production values is observed across different parts. The highest production values, approximately 9 MJ, are concentrated in the northern and central parts of the study area. However, in the southern regions, production levels decrease to below 2 MJ. When comparing two cases, Case 1 demonstrates higher methane production levels across

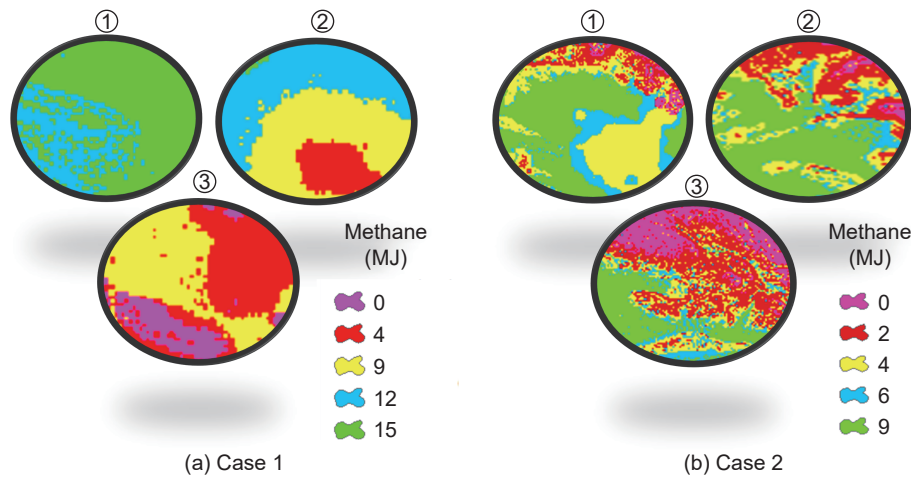


Fig. 5 Methane performance per year. Study area: ① northern, ② central, and ③ southern.

the study area compared to Case 2.

(2) Tar and char

Tar and char values derived from the gasification process are computed using Eqs. (17) and (18). As depicted in Table 5, the maximum tar production for Case 1 is recorded at 24.04 t/ha, whereas for Case 2, it stands at 19.67 t/ha. Conversely, the lowest tar production for Cases 1 and 2 is noted as 0 t/ha. Furthermore, the highest char production for Case 1 is observed at 21.75 t/ha, whereas for Case 2, it amounts to 17.20 t/ha.

(3) CO₂

Although in the process of gasification, the production of CO₂ gas can have challenges for the environment, but it can be converted into a cleaner product, such as urea during a process. Equation (19) is

Table 5 Tar and char production in different cases.

Case	Tar production (t/ha)	Char production (t/ha)
Case 1 (low)	0	0
Case 1 (high)	24.04	21.75
Case 2 (low)	0	0
Case 2 (high)	19.67	17.20

used to estimate the amount of CO₂ produced during the gasification process. One of the goals of this research is to reduce air pollution by preventing the re-emission of CO₂ and turning it into a valuable fertilizer, especially urea, which has been emphasized by Ref. [61]. The results presented in Table 6 show the estimated annual production of urea fertilizers for both cases. By adopting this method, the gasification process acts as a dual-purpose solution, simultaneously reducing air pollution caused by CO₂ emissions and providing a cleaner product.

The hydrogen production levels resulting from the gasification process between 1988 and 2021, alongside the maximum biomass concentration in the northern regions of Case 1 and the western part of Case 2, are depicted in Fig. 6, which illustrates the trends in hydrogen (H₂) production, with each year exhibiting distinct characteristics.

It is important to note that, in Case 1, the highest hydrogen yield potential was 261.54 MJ/ha in 2016, while the lowest was 139.5 MJ/ha in 2012. Similarly, in Case 2, hydrogen production reached its peak at 192.5 MJ/ha in 2002. Conversely, the lowest hydrogen production was observed in 2012 at 166.5 MJ/ha.

Table 6 Urea amount.

						(t/ha)					
Year	Case 1	Case 2	Year	Case 1	Case 2	Year	Case 1	Case 2	Year	Case 1	Case 2
1998	7.42	5.97	2004	7.26	7.05	2010	7.41	8.13	2016	7.42	10.47
1999	7.51	6.15	2005	7.40	7.23	2011	7.35	9.01	2017	7.21	8.65
2000	7.36	5.41	2006	7.25	7.41	2012	6.67	5.59	2018	7.37	9.57
2001	7.41	6.51	2007	7.03	7.03	2013	7.29	9.91	2019	7.29	9.01
2002	7.71	7.21	2008	7.42	7.77	2014	7.42	8.85	2020	7.42	9.93
2003	7.37	5.97	2009	7.16	6.49	2015	7.41	9.03	2021	7.51	9.75

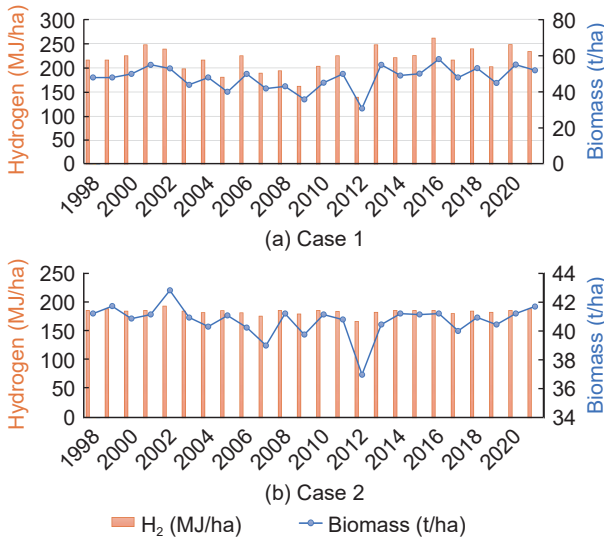


Fig. 6 Amount of produced hydrogen from 1998 to 2021.

3.5 Correlation between climate parameters and hydrogen production

As illustrated in Fig. 2, climatic parameters exhibit a greater impact on biomass and consequently hydrogen

production compared to soil parameters. Figure 7 depicts Pearson’s correlation results to show relationship between climate parameters and hydrogen production levels.

3.6 Electricity generation assessment from hydrogen

In this section, a comprehensive analysis of hydrogen production, area, and electrical energy generation across four samples points in Case 2 are provided in Fig. 8. Box plots in Fig. 8a, represent the range of hydrogen production values for each sample, with sample *a* having the highest average production, followed by samples *b*, *c*, and *d*. The variability within each sample is relatively small which indicates the hydrogen potential in those samples. Also, Fig. 8b shows the distribution of area (in ha) associated with each sample. Based on Fig. 8b, sample *a* has the largest area, followed by samples *b* and *d*, while sample *c* has the smallest area. This distribution suggests that sample *a* covers a significantly larger land area, which may correlate with a higher potential for hydrogen

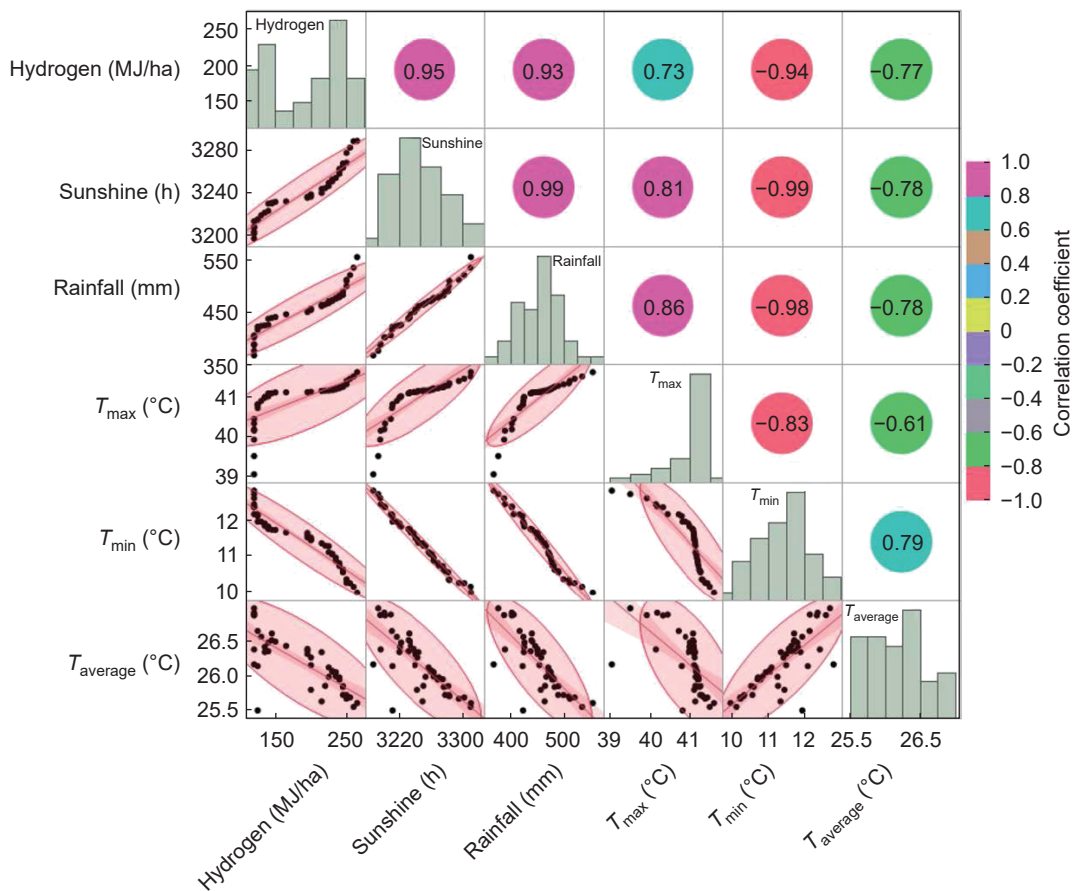


Fig. 7 Correlation between climatic parameters.

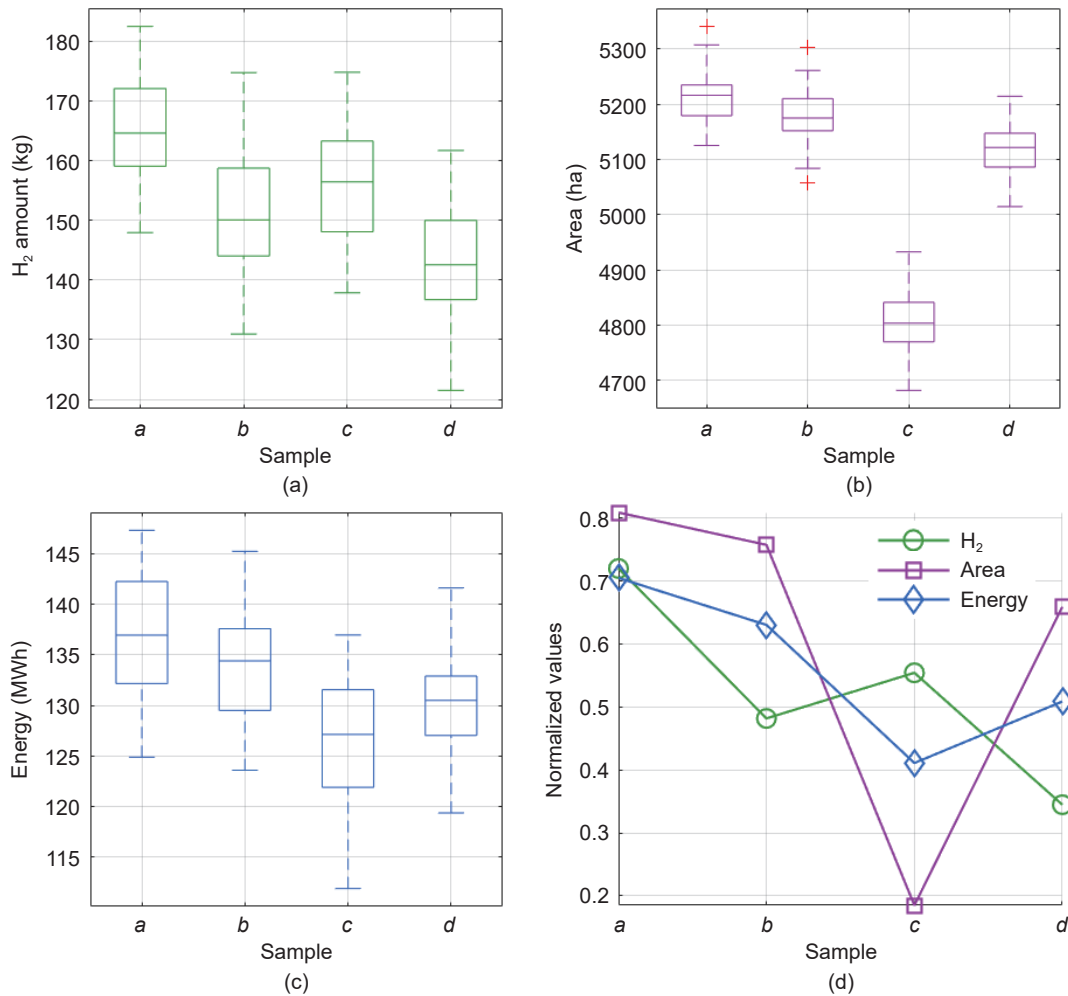


Fig. 8 Boxplots and normalized data comparison of hydrogen production, area, and generated electrical energy across four samples (a, b, c, and d).

production and energy generation. Moreover, Fig. 8c depicts the generated electrical energy (in MWh) for each sample. Sample *a* shows the highest average energy generation, while sample *c* shows the lowest median value. However, all samples exhibit similar variability in terms of energy generation, indicating that while overall energy production differs, energy efficiency remains relatively consistent across the samples. Finally, Fig. 8d provides a more complex analysis by normalizing the data of hydrogen production, area, and generated electrical energy.

In order to develop a comprehensive big data green system that closely mirrors real-world conditions, future work should prioritize new, robust, and cost-effective frameworks. Utilizing multi-UAV systems could be key, as they offer continuous, affordable data collection and can quickly update information as needed for improved management^[62, 63]. In fact,

providing key data through the Internet of Things (IoT) is an advanced approach to modernizing data-driven systems^[64]. While multi-UAVs can capture remote telephoto images, some challenges remain and should be addressed in future studies^[65]. Moreover, if each section of the case study has its own policymaker, commercial aspects must be carefully considered. This includes ensuring privacy preservation, as policymakers may be unwilling to share all critical information^[66]. Therefore, it is recommended to leverage findings from existing research to address this challenge effectively^[67].

Future research should also focus on integrating biomass-based hydrogen production with renewable energy sources to enhance overall system efficiency and sustainability. Investigating advanced storage methods, including seasonal hydrogen storage solutions, and leveraging machine learning algorithms

for predictive analytics and optimization are promising directions. Moreover, combining these efforts with cloud-based big data computing can provide enhanced scalability and real-time decision-making capabilities to ensure a more robust and efficient hydrogen production and distribution framework. Given the region's vulnerability to natural hazards, such as droughts and floods, which can impact biomass availability and hydrogen production efficiency, future studies should also consider mapping high-risk areas. Excluding these areas from planning can improve the resilience and sustainability of biomass-based energy systems.

4 Conclusion

This study presents significant advancements in utilizing biomass for hydrogen production through gasification. A comprehensive framework is developed to evaluate the regional suitability for biomass-derived hydrogen production across different climates, using spatial big data analysis combined with fuzzy-BWM method. Two different climate zones in southern Iran are analyzed to assess the hydrogen production potential with the proposed framework. The fuzzy-BWM method effectively addresses the multi-criteria decision-making process in determining proper weight for each input parameters. The study highlights that spatial assessment combined with interpolation techniques is a vital step to assess the potential of each region. In the moderate climate, the highest hydrogen production is 254 MJ/ha, while in the semi-arid climate, it is lower, peaking at 190 MJ/ha. This indicates that moderate climates can yield up to 26% more hydrogen production compared to semi-arid regions. Additionally, byproducts, such as methane, tar, and char, can be managed and utilized beneficially.

Acknowledgment

This work was supported by the Guangdong Major Project of Basic and Applied Basic Research (No. 2023B0303000009). The authors thank Dr. M. Khosravi and Dr. Y. Cui for their scientific management and contribution.

References

- [1] M. A. Alghamdi, A. S. AL-Malaise AL-Ghamdi, and M. Ragab, Predicting energy consumption using stacked LSTM snapshot ensemble, *Big Data Mining and Analytics*, vol. 7, no. 2, pp. 247–270, 2024.
- [2] F. Durante, A. Gianfreda, F. Ravazzolo, and L. Rossini, A multivariate dependence analysis for electricity prices, demand and renewable energy sources, *Inf. Sci.*, vol. 590, pp. 74–89, 2022.
- [3] P. Wang, X. Dong, J. Chen, X. Wu, and F. Chiclana, Reliability-driven large group consensus decision-making method with hesitant fuzzy linguistic information for the selection of hydrogen storage technology, *Inf. Sci.*, vol. 689, p. 121457, 2025.
- [4] C. Acar and I. Dincer, Review and evaluation of hydrogen production options for better environment, *J. Cleaner Prod.*, vol. 218, pp. 835–849, 2019.
- [5] X. Zhang, C. Xia, M. S. AlSalhi, S. Devanesan, M. Sekar, G. Jhanani, S. Kandasamy, and H. Li, Assessments of the power production, energy consumption and emission comparison of hydrogen feed vehicles, *Fuel*, vol. 334, p. 126794, 2023.
- [6] Z. Fan, W. Weng, J. Zhou, D. Gu, and W. Xiao, Catalytic decomposition of methane to produce hydrogen: A review, *J. Energy Chem.*, vol. 58, pp. 415–430, 2021.
- [7] M. Younas, S. Shafique, A. Hafeez, F. Javed, and F. Rehman, An overview of hydrogen production: Current status, potential, and challenges, *Fuel*, vol. 316, p. 123317, 2022.
- [8] J. L. C. Fajín and M. N. D. S. Cordeiro, Renewable hydrogen production from biomass derivatives or water on trimetallic based catalysts, *Renew. Sustain. Energy Rev.*, vol. 189, p. 113909, 2024.
- [9] M. Li, H. Wang, and J. Li, Mining conditional functional dependency rules on big data, *Big Data Mining and Analytics*, vol. 3, no. 1, pp. 68–84, 2020.
- [10] M. S. Rahman and H. Reza, A systematic review towards big data analytics in social media, *Big Data Mining and Analytics*, vol. 5, no. 3, pp. 228–244, 2022.
- [11] Y. Zhao, J. Zhao, and E. Y. Lam, House price prediction: A multi-source data fusion perspective, *Big Data Mining and Analytics*, vol. 7, no. 3, pp. 603–620, 2024.
- [12] X. Sun, Y. He, D. Wu, and J. Z. Huang, Survey of distributed computing frameworks for supporting big data analysis, *Big Data Mining and Analytics*, vol. 6, no. 2, pp. 154–169, 2023.
- [13] Z. Wang, B. Chen, J. Wang, J. Kim, and M. M. Begovic, Robust optimization based optimal DG placement in microgrids, *IEEE Trans. Smart Grid*, vol. 5, no. 5, pp. 2173–2182, 2014.
- [14] D. Gautam and N. Mithulananthan, Optimal DG placement in deregulated electricity market, *Electric Power Syst. Res.*, vol. 77, no. 12, pp. 1627–1636, 2007.
- [15] U. Sultana, A. B. Khairuddin, M. M. Aman, A. S. Mokhtar, and N. Zareen, A review of optimum DG placement based on minimization of power losses and voltage stability enhancement of distribution system, *Renew. Sustain. Energy Rev.*, vol. 63, pp. 363–378, 2016.
- [16] S. Beck and D. Fischer, A methodological framework for geospatial modelling of hydrogen demand in cities, *Energy Inf.*, vol. 6, no. S1, p. 21, 2023.
- [17] L. A. Müller, A. Leonard, P. A. Trotter, and S. Hirmer, Green hydrogen production and use in low- and middle-

- income countries: A least-cost geospatial modelling approach applied to Kenya, *Appl. Energy*, vol. 343, p. 121219, 2023.
- [18] M. Khosravi, H. Parsaei, K. Rezaee, and M. S. Helfroush, Fusing convolutional learning and attention-based bi-LSTM networks for early Alzheimer's diagnosis from EEG signals towards IoMT, *Sci. Rep.*, vol. 14, no. 1, p. 26002, 2024.
- [19] M. Khosravi, H. Parsaei, and K. Rezaee, Novel classification scheme for early Alzheimer's disease (AD) severity diagnosis using deep features of the hybrid cascade attention architecture: Early detection of AD on MRI Scans, *Tsinghua Science and Technology*, vol. 30, no. 6, pp. 2572–2591, 2025.
- [20] G. P. Shukla, S. Kumar, S. K. Pandey, R. Agarwal, N. Varshney, and A. Kumar, Diagnosis and detection of Alzheimer's disease using learning algorithm, *Big Data Mining and Analytics*, vol. 6, no. 4, pp. 504–512, 2023.
- [21] M. Wang, R. Yao, and K. Rezaee, Mu-net-optLSTM: Two-stream spatial-temporal feature extraction and classification architecture for automatic monitoring of crowded art museums, *Tsinghua Science and Technology*, doi: 10.26599/TST.2024.9010003.
- [22] M. J. Mokarram, M. Mokarram, M. Khosravi, and Y. Cui, Optimizing risk control for solar farm green management using DNI estimation at the edge through a GLE-SVR learning model, *Tsinghua Science and Technology*, doi: 10.26599/TST.2024.9010171.
- [23] F. Tavassolian, M. Abbasi, A. Ramezani, A. Taherkordi, and M. R. Khosravi, ResFed: An accurate and light federated multi-shot pre-trained model on edge devices, *Tsinghua Science and Technology*, vol. 30, no. 4, pp. 1539–1551, 2025.
- [24] D. Panchal, P. Chatterjee, R. Sharma, and R. K. Garg, Sustainable oil selection for cleaner production in Indian foundry industries: A three phase integrated decision-making framework, *J. Cleaner Prod.*, vol. 313, p. 127827, 2021.
- [25] D. Wanyama, M. Mighty, S. Sim, and F. Koti, A spatial assessment of land suitability for maize farming in Kenya, *Geocarto Int.*, vol. 36, no. 12, pp. 1378–1395, 2021.
- [26] D. Jorge-García and V. Estruch-Guitart, Comparative analysis between AHP and ANP in prioritization of ecosystem services—A case study in a rice field area raised in the Guadalquivir marshes (Spain), *Ecol. Inf.*, vol. 70, p. 101739, 2022.
- [27] H. Q. Nguyen, V. T. Nguyen, D. P. Phan, Q. H. Tran, and N. P. Vu, Multi-criteria decision making in the PMEDM process by using MARCOS, TOPSIS, and MAIRCA methods, *Appl. Sci.*, vol. 12, no. 8, p. 3720, 2022.
- [28] D. Pamučar, F. Ecer, G. Cirovic, and M. A. Arlasheedi, Application of improved best worst method (BWM) in real-world problems, *Mathematics*, vol. 8, no. 8, p. 1342, 2020.
- [29] M. Krstić, S. Tadić, and L. Agnusdei, Evaluating governance models in intermodal terminal operations: A hybrid grey MCDM approach, *J. Intell. Manage. Decis.*, vol. 2, no. 4, pp. 179–191, 2023.
- [30] P. C. Y. Liu, H. W. Lo, and J. J. H. Liou, A combination of DEMATEL and BWM-based ANP methods for exploring the green building rating system in Taiwan, *Sustainability*, vol. 12, no. 8, p. 3216, 2020.
- [31] M. Akbari, S. G. Meshram, R. S. Krishna, B. Pradhan, S. Shadeed, K. M. Khedher, M. Sepehri, A. R. Ildoromi, F. Alimerzaei, and F. Darabi, Identification of the groundwater potential recharge zones using MCDM models: Full consistency method (FUCOM), best worst method (BWM) and analytic hierarchy process (AHP), *Water Resour. Manage.*, vol. 35, no. 14, pp. 4727–4745, 2021.
- [32] C. C. Yang, C. C. Shen, T. Y. Mao, H. W. Lo, and C. J. Pai, A hybrid model for assessing the performance of medical tourism: Integration of Bayesian BWM and Grey PROMETHEE-AL, *J. Funct. Spaces*, vol. 2022, p. 5745499, 2022.
- [33] S. H. H. Petrudi, H. Ghomi, and M. Mazaheriasad, An integrated fuzzy Delphi and best worst method (BWM) for performance measurement in higher education, *Decis. Anal. J.*, vol. 4, p. 100121, 2022.
- [34] M. Mokarram, J. Aghaei, M. J. Mokarram, G. P. Mendes, and B. Mohammadi-Ivatloo, Geographic information system-based prediction of solar power plant production using deep neural networks, *IET Renew. Power Gener.*, vol. 17, no. 10, pp. 2663–2678, 2023.
- [35] Q. Meng, Z. Liu, and B. E. Borders, Assessment of regression kriging for spatial interpolation—comparisons of seven GIS interpolation methods, *Cartogr. Geogr. Inf. Sci.*, vol. 40, no. 1, pp. 28–39, 2013.
- [36] A. Drewnowski and I. Kawachi, Diets and health: How food decisions are shaped by biology, economics, geography, and social interactions, *Big Data*, vol. 3, no. 3, pp. 193–197, 2015.
- [37] L. Qu, H. Lu, Z. Tian, J. M. School, B. Huang, Y. Liang, D. Qiu, and Y. Liang, Spatial prediction of soil sand content at various sampling density based on geostatistical and machine learning algorithms in plain areas, *CATENA*, vol. 234, p. 107572, 2024.
- [38] P. Kumar, B. Rao, A. Burman, S. Kumar, and P. Samui, Spatial variation of permeability and consolidation behaviors of soil using ordinary kriging method, *Groundwater Sustain. Dev.*, vol. 20, p. 100856, 2023.
- [39] M. Mokarram, H. R. Pourghasemi, K. Huang, and H. Zhang, Investigation of water quality and its spatial distribution in the Kor River basin, Fars province, Iran, *Environ. Res.*, vol. 204, p. 112294, 2022.
- [40] Y. Dong, R. Chen, E. Petropoulos, B. Yu, J. Zhang, X. Lin, M. Gao, and Y. Feng, Interactive effects of salinity and SOM on the coenzymatic activities across coastal soils subjected to a saline gradient, *Geoderma*, vol. 406, p. 115519, 2022.
- [41] Q. Chen, B. Niu, Y. Hu, T. Luo, and G. Zhang, Warming and increased precipitation indirectly affect the composition and turnover of labile-fraction soil organic matter by directly affecting vegetation and

- microorganisms, *Sci. Total Environ.*, vol. 714, p. 136787, 2020.
- [42] M. Mokarram, M. J. Mokarram, M. Gitizadeh, T. Niknam, and J. Aghaei, A novel optimal placing of solar farms utilizing multi-criteria decision-making (MCDA) and feature selection, *J. Cleaner Prod.*, vol. 261, p. 121098, 2020.
- [43] Y. Zhao, Y. Xu, S. Yüksel, H. Dinçer, and G. G. Ubay, Hybrid IT2 fuzzy modelling with alpha cuts for hydrogen energy investments, *Int. J. Hydrogen Energy*, vol. 46, no. 13, pp. 8835–8851, 2021.
- [44] S. Kheybari and A. Ishizaka, The behavioural best-worst method, *Expert Syst. Appl.*, vol. 209, p. 118265, 2022.
- [45] A. Hashemizadeh, Y. Ju, and P. Dong, A combined geographical information system and best-worst method approach for site selection for photovoltaic power plant projects, *Int. J. Environ. Sci. Technol.*, vol. 17, no. 4, pp. 2027–2042, 2020.
- [46] J. Rezaei, Best-worst multi-criteria decision-making method, *Omega*, vol. 53, pp. 49–57, 2015.
- [47] L. Liu, P. Jiang, H. Qian, L. Mu, X. Lu, and J. Zhu, CO₂-negative biomass conversion: An economic route with co-production of green hydrogen and highly porous carbon, *Appl. Energy*, vol. 311, p. 118685, 2022.
- [48] S. Valizadeh, H. Hakimian, A. Farooq, B. H. Jeon, W. H. Chen, S. H. Lee, S. C. Jung, M. W. Seo, and Y. K. Park, Valorization of biomass through gasification for green hydrogen generation: A comprehensive review, *Bioresour. Technol.*, vol. 365, p. 128143, 2022.
- [49] H. Song, G. Yang, P. Xue, Y. Li, J. Zou, S. Wang, H. Yang, and H. Chen, Recent development of biomass gasification for H₂ rich gas production, *Appl. Energy Combust. Sci.*, vol. 10, p. 100059, 2022.
- [50] S. Mishra and R. K. Upadhyay, Review on biomass gasification: Gasifiers, gasifying mediums, and operational parameters, *Mater. Sci. Energy Technol.*, vol. 4, pp. 329–340, 2021.
- [51] M. Buffi, M. Prussi, and N. Scarlat, Energy and environmental assessment of hydrogen from biomass sources: Challenges and perspectives, *Biomass Bioenergy*, vol. 165, p. 106556, 2022.
- [52] S. Samanta, D. Roy, S. Roy, A. Smallbone, and A. P. Roskilly, Modelling of hydrogen blending into the UK natural gas network driven by a solid oxide fuel cell for electricity and district heating system, *Fuel*, vol. 355, p. 129411, 2024.
- [53] J. J. Hwang, Effect of hydrogen delivery schemes on fuel cell efficiency, *J. Power Sources*, vol. 239, pp. 54–63, 2013.
- [54] K. Mishra, S. S. Siwal, A. K. Saini, and V. K. Thakur, Recent update on gasification and pyrolysis processes of lignocellulosic and algal biomass for hydrogen production, *Fuel*, vol. 332, p. 126169, 2023.
- [55] H. Saboori and R. Hemmati, Considering carbon capture and storage in electricity generation expansion planning, *IEEE Trans. Sustain. Energy*, vol. 7, no. 4, pp. 1371–1378, 2016.
- [56] X. Wu, H. Li, X. Wang, and W. Zhao, Cooperative operation for wind turbines and hydrogen fueling stations with on-site hydrogen production, *IEEE Trans. Sustain. Energy*, vol. 11, no. 4, pp. 2775–2789, 2020.
- [57] Ö. Tezer, N. Karabağ, A. Öngen, C. Ö. Çolpan, and A. Ayol, Biomass gasification for sustainable energy production: A review, *Int. J. Hydrogen Energy*, vol. 47, no. 34, pp. 15419–15433, 2022.
- [58] J. M. Clairand, M. Arriaga, C. A. Cañizares, and C. Álvarez-Bel, Power generation planning of Galapagos' microgrid considering electric vehicles and induction stoves, *IEEE Trans. Sustain. Energy*, vol. 10, no. 4, pp. 1916–1926, 2019.
- [59] E. A. Byers, G. Coxon, J. Freer, and J. W. Hall, Drought and climate change impacts on cooling water shortages and electricity prices in Great Britain, *Nat. Commun.*, vol. 11, no. 1, p. 2239, 2020.
- [60] X. Li, C. J. Raorane, C. Xia, Y. Wu, T. K. N. Tran, and T. Khademi, Latest approaches on green hydrogen as a potential source of renewable energy towards sustainable energy: Spotlighting of recent innovations, challenges, and future insights, *Fuel*, vol. 334, p. 126684, 2023.
- [61] K. Hasler, S. Bröring, O. S. W. F. Omta, and H. W. Olf, Eco-innovations in the German fertilizer supply chain: Impact on the carbon footprint of fertilizers, *Plant Soil Environ.*, vol. 63, no. 12, pp. 531–544, 2017.
- [62] Y. Cui, L. Cheng, M. Basin, and Z. Wu, Distributed Byzantine-resilient learning of multi-UAV systems via filter-based centerpoint aggregation rules, *IEEE/CAA J. Autom. Sin.*, vol. 12, no. 5, pp. 1056–1058, 2025.
- [63] J. Gao, J. Zhang, X. Xu, L. Qi, Y. Yuan, Z. Li, and W. Dou, Energy-efficient task offloading in UAV-enabled MEC via multi-agent reinforcement learning, in *Proc. 18th Int. Conf. Green, Pervasive, and Cloud Computing*, Harbin, China, 2023, pp. 63–80.
- [64] C. Hu, W. Fan, E. Zeng, Z. Hang, F. Wang, L. Qi, and M. Z. A. Bhuiyan, Digital twin-assisted real-time traffic data prediction method for 5G-enabled internet of vehicles, *IEEE Trans. Ind. Inf.*, vol. 18, no. 4, pp. 2811–2819, 2021.
- [65] Y. Cui, Y. Huang, M. V. Basin, and Z. Wu, Geometric programming for nonlinear satellite buffer networks with time delays under L1-gain performance, *IEEE/CAA J. Autom. Sin.*, vol. 11, no. 2, pp. 554–556, 2024.
- [66] L. Qi, R. Wang, C. Hu, S. Li, Q. He, and X. Xu, Time-aware distributed service recommendation with privacy-preservation, *Inf. Sci.*, vol. 480, pp. 354–364, 2019.
- [67] F. Fei, S. Li, H. Dai, C. Hu, W. Dou, and Q. Ni, A K-anonymity based schema for location privacy preservation, *IEEE Trans. Sustain. Comput.*, vol. 4, no. 2, pp. 156–167, 2019.



Mohammad Jafar Mokarram holds a PhD in electrical power engineering and is currently a postdoctoral researcher at Shenzhen University, China. His research focuses on power networks, renewable energies, and the integration of artificial intelligence in energy systems. He has contributed to several key projects in these fields to advance sustainable energy solutions.



Arsalan Najafi received the BEng degree in electrical engineering from University of Kurdistan, Sanandaj, Iran in 2009, and the MEng and PhD degrees in electrical engineering from University of Birjand, Birjand, Iran in 2011 and 2016, respectively. He won the grant of the Polish National Agency for Academic Exchange (NAWA) under the Ulam Program grant in 2021 to commence his postdoctoral research in multi-energy systems. His journey in academia has been marked by transitioning from a postdoctoral researcher to an assistant professor at Wroclaw University of Science and Technology, Poland. He is currently a postdoctoral researcher at Department of Architecture and Civil Engineering, Chalmers University of Technology, Sweden. His commitment to academia and research extends into his pursuit of innovative solutions in multi-energy systems, with a particular focus on transportation electrification, electricity markets, and optimization theory in energy systems.



Jamsid Aghaei received the BEng degree in electrical engineering from Power and Water Institute of Technology, Tehran, Iran in 2003, and the MEng and PhD degrees from Iran University of Science and Technology, Tehran, Iran in 2005 and 2009, respectively. He is currently a full-time professor at Central Queensland University, Rockhampton, Australia, with a research focus on smart grids, renewable energy systems, electricity markets, and power system operation, optimization, and planning. He serves as an associate editor for *IEEE Transactions on Smart Grid*, *IEEE Systems Journal*, and *IET Renewable Power Generation*, and a subject editor for *IET Generation, Transmission & Distribution*. In 2017, he was recognized as an outstanding reviewer for *IEEE Transactions on Sustainable Energy*. He is a senior member of IEEE.



Meng Yuan received the MEng degree from Wuhan University, China in 2016, and subsequently joined College of Mechatronics and Control Engineering, Shenzhen University, China. She is also a PhD candidate at The University of Hong Kong, China, with research interests in reinforcement learning based optimization, large language models, and social network analysis grounded in complex network theory.